Fracture in high performance fibre reinforced concrete road pavement materials.

Erik Denneman[a,1], Rongzong Wu[b], Elsabe P. Kearsley[c], Alex T. Visser[c]

[a] University of California Pavement Research Center, 1353 South 46th Street, Bldg. 452, Richmond, CA 94804, USA. Corresponding author, Tel: +27-12-841-2933; fax: +27-12-841-2081, E-mail address: edenneman@csir.co.za

[b] University of California Pavement Research Center, 1353 South 46th Street, Bldg. 452, Richmond, CA 94804, USA.

[c] Dept of Civil Engineering, University of Pretoria, Pretoria, 0002, South Africa

Abstract

In this paper a simple, but effective methodology to simulate opening mode fracture in high performance fibre reinforced concrete is presented. To obtain the specific fracture energy of the material, load-deflection curves from three point bending (TPB) experiments are extrapolated. The proposed extrapolation technique is an adaptation of an approach originally developed for plain concrete. The experimental part of the paper includes a size effect study on TPB specimens. The post crack behaviour of the material is modelled using a cohesive softening function with crack tip singularity. Numerical simulation of the experiments is performed by means of an embedded discontinuity method. The simulation provides satisfactory predictions of the fracture behaviour of the material and the size-effect observed in the experiments.

---

[1] Permanent address: CSIR Built Environment, Meiring Naudé Road, Pretoria, 0184, South Africa

Keywords

Fibre reinforced materials, concrete, embedded discontinuity method, crack tip singularity, civil engineering structures.

Abbreviations

CMOD   Crack mouth opening displacement

EDM: Embedded discontinuity method

MOR: Modulus of rupture

TPB*:*   Three point bending

UTCRCP   Ultra-thin continuously reinforced concrete pavement

Nomenclature

a:	Notch depth	[mm]
A:	Empirical constant	[N]
b:	Width of specimen	[mm]
E:	Modulus of elasticity	[GPa]
f_c	Compressive strength	[MPa]
f_t:	Tensile strength	[MPa]
G_f:	Fracture energy	[N/mm]
h:	Height of specimen	[mm]
L:	Specimen length	[mm]
P:	Load	[N]
P_u:	Peak load	[N]

s:	Span	[mm]
W_f	Work of fracture	[Nmm]
W_{tail}	Work of fracture under modelled P-δ tail	[Nmm]
w:	Crack width	[mm]
y:	Position along vertical axis of beam	[mm]
δ	Deflection at midspan	[mm]
v:	Poisson's ratio	
σ:	Crack bridging stress	[MPa]
σ_{Nu}	Nominal tensile strength	[MPa]
φ	Angle of rotation	[rad]

1. Introduction

Unlike other fields of engineering, the adoption of fracture mechanics in civil engineering practice has been slow. A strong case for the use of fracture mechanics can be made however, in particular for the design of concrete structures, since concrete exhibits considerable size effects in fracture [1]. A reason for the slow adoption may be the perceived complexity associated with design using fracture mechanics approaches and the specialized testing involved.

The materials under study in this paper are high performance concrete mixes developed for use in an innovative pavement system known as Ultra-Thin Continuously Reinforced Concrete Pavement (UTCRCP). A key parameter in the design of UTCRCP is the nominal tensile strength (σ_{Nu}). σ_{Nu} is determined from the peak load recorded in bending tests on beams, assuming a linear elastic stress distribution. Earlier work has shown σ_{Nu} for the UTCRCP material to be subject to significant size effects [2]. As a consequence, generalizing the σ_{Nu} value obtained from beam bending tests to the

design of three dimensional pavement structures is problematic. To overcome the size-effect problem, a need exists to develop reliable, but simple, fracture mechanics based method to predict the structural performance of UTCRCP material in bending.

The objective of the paper is to numerically simulate mode I (opening mode) fracture in high performance fibre reinforced concrete. To enable numerical simulation, the fracture energy of the material needs to be determined. A methodology is proposed to accurately measure the full work of fracture (W_f) required to break fibre reinforced concrete specimens in three point bending (TPB) tests. From W_f, the specific fracture energy (G_f) of the material is determined. G_f is used in the definition of a softening function with crack tip singularity. The cohesive crack relation for the material thus obtained allows simulation of the fracture behaviour observed in TPB tests. The experimental programme for this study includes TPB specimens of different sizes produced from two UTCRCP mix designs. Numerical simulation is performed with an Embedded Discontinuity Method (EDM) implemented in an open source finite element framework.

2. Determining the fracture energy of fibre reinforced concrete from TPB tests

The work of fracture (W_f) required to completely break a specimen in a TPB test is represented by the area under the load-deflection (P-δ) curve, or load-crack mouth opening displacement (CMOD) curve. The deflection (δ) is the vertical displacement at midspan measured during the experiments. The CMOD is gauged over the mouth of the notch in TPB tests on pre-notched samples. In the experiments performed as part of this study both δ and CMOD were recorded. Figure 1a shows the load-deflection curves obtained for a group of specimens tested. A schematic representation of the TPB test configuration is shown in Figure 1b.

The energy required to produce a unit of fractured area G_f, is calculated for the concrete-fibres composite material using Equation 1.

$$G_f = \frac{W_f}{b(h-a)}$$ (1)

where b is the width of the sample, h the total sample height and a the notch depth. In this calculation it is assumed that the effect of fibre reinforcement is distributed equally over the ligament area. The composite fibre concrete material behaves as a homogeneous material and the fibres do not need to be modelled as separate entities.

The fibre reinforced concrete under study behaves ductile when compared to plain concrete. To obtain the full work of fracture from the TPB tests, the specimens need to be broken completely. This requires all steel fibres in the ligament area to be pulled out right to the top of the beam. For the 30 mm long steel fibres used in this study this would require a theoretical crack width of 15 mm at the top of the beam. The large rotation of the two beam halves needed to achieve this cannot be reached in the normal TPB test setup. TPB tests on fibre reinforced concrete will therefore generally be stopped before the beam is fully broken. As a result, a part of the tail of the load-deflection curve will be missing, as can be observed in Figure 1. The figure shows that after the peak load is reached, the load reduces asymptotically towards zero with the further increase of deflection. At the final stage of the experiment the load has reduced significantly, but the specimens have not broken completely into two halves and the full work of fracture has therefore not been recorded.

To calculate the full work of fracture and get a precise measure of G_f, it will be necessary to model the missing part of the load-deflection curve. A methodology is proposed that draws from an extrapolation technique developed for plain concrete by Elices et al [3], [4], Bažant and Planas [1] and Roselló et al [5].

Near the end of the bending test, the crack has propagated to the top of the beam and the crack mouth has opened considerably. The neutral axis of the stress distribution shifts ever closer to top of the beam as the size of the compressive zone reduces during the test. In this situation, the beam can be modelled as two ridged parts rotating around a point at the top of the beam at centre span, as shown in Figure 2a. For fibre reinforced concrete this situation will exists for a considerable longer period than for plain concrete, while the fibres bridging the crack are being pulled out. The angle of rotation (φ) around the hinge point at the top of the beam at any value of δ is obtained from:

$$\tan \varphi = \frac{2\delta}{s} \Rightarrow \varphi \approx \frac{2\delta}{s} \tag{2}$$

The crack width at any depth y of the beam near the end of the test is calculated from:

$$w_y = 2y \sin \varphi \approx 2y\varphi \tag{3}$$

It can be shown that the kinematic model of the beam in Figure 2a is accurate, by comparing the horizontal crack opening displacement at the mouth of the notch calculated using the model, to the CMOD measured with a clip gauge for tests in which both the CMOD and vertical displacement were recorded. At large rotations the recorded CMOD and the crack mouth opening calculated using the kinematic model in Figure 2a reach unity:

$$\frac{2h \sin \varphi}{CMOD} = 1 \tag{4}$$

For the beam data shown in Figure 3, unity is reached at approximately 2 mm deflection, implying that from this point onward the kinematic model is valid for the data. The stress distribution in the beam at large rotations may be approximated by assuming that the depth of the compressive zone is negligible and concentrated at the hinge point [3]. The post crack softening behaviour of the material can be described using a cohesive crack approach as introduced for concrete by Hillerborg

et al [6]. Under the assumption of a cohesive crack, the material behaves elastically until the stress reaches the tensile strength (f_t) of the material. At this point a crack is formed. Stresses are transferred over the crack according to a softening function. The crack bridging tensile stress (σ_y) at any point y along the depth of the cracked beam shown in Figure 2b is written as a function of the crack width (w_y) at that position:

$$\sigma_y = \mathrm{f}(w_y) \tag{5}$$

Regardless of the shape of the softening function, the moment capacity in the kinematic model can be written as the integral of the softening function times the lever arm to the top of the beam:

$$M = \int_0^h \sigma(w_y) b y\, \mathrm{d}y \tag{6}$$

Substituting w_y in Equation 6 by the relation in Equation 3 results in:

$$M = \frac{b}{(2\varphi)^2} \int_0^{w_c} \sigma(w_y) w_y\, \mathrm{d}w \tag{7}$$

where w_c is the crack width opening position at which the softening is complete and $\sigma = 0$. Note that for exponential softening $w_c = \infty$. Following Elices et al [3], the integral in Equation 7 is defined as parameter A:

$$A = \int_0^{w_c} \sigma(w_y) w_y \mathrm{d}w \tag{8}$$

With this, Equation 7 may be written as:

$$\frac{M}{b} = \frac{A}{(2\varphi)^2} \tag{9}$$

This defines a relationship between the remaining moment capacity M in the beam at large displacements, and the angle of rotation φ. Parameter A can be calculated without having to define the shape of the softening curve, as A corresponds to the slope of a graph plotting M/b against $(2\varphi)^{-2}$. The behaviour of parameter A at large rotations (small values of $(2\varphi)^{-2}$), where it becomes a constant, is shown in Figure 4 for data obtained from TPB tests performed as part of this study. A is determined per specimen type using least squares fitting.

Once A has been determined the missing part of the asymptotic tail of the displacement curve can be modelled by combining Equations 2 and 9 which allows calculation of P_{tail} for any δ.

$$P_{tail} = \frac{bsA}{4\delta^2} \tag{10}$$

Figure 5 shows an example of a load-deflection curve with a modelled tail end. The modelled tail provides a close fit to the path of the experimental tail, and can be used to extrapolate the load-deflection curve to infinity. The total work of fracture can now be calculated by adding the area under the modelled tail of the curve to the area under the known part of the curve. The work under the modelled tail is determined from:

$$W_{tail} = \int_{\delta_{end}}^{\infty} P \mathrm{d}(\delta) = \frac{bsA}{4\delta_{end}} \tag{11}$$

Where, δ_{end} is the deflection at the last available experimental data point. The total W_f can now be calculated by adding W_{tail} to the area under the experimental load-deflection curve. Finally, G_f can be determined from Equation 1. G_f represents the area under the softening function used in the next section to model the post crack behaviour of the material.

3. Numerical simulation of fracture behaviour of fibre reinforced concrete

3.1 Embedded discontinuity method

The numerical simulation of fracture in the high performance fibre reinforced concrete material is performed using an embedded discontinuity method (EDM). The approach is based on the work by Simo et al [7], Oliver [8], [9] and Sancho et al [10]. The EDM code used for this paper was implemented into the open source finite element method (FEM) software framework OpenSees [11] by Wu et al [12].

The embedded discontinuity method (EDM) takes its name from embedding a strong discontinuity within finite elements. It is one of the techniques available to implement the strong discontinuity approach (SDA). A strong discontinuity is typified by "*the occurrence jumps in the displacement field appearing at a certain time, in general unknown before the analysis, of the loading history and developing across paths of the solid which are material (fixed) surfaces*" [8]. Essentially, EDM adds internal nodes to cracked elements. The extra degrees of freedom associated with these internal nodes are used to describe the displacement jumps (both in shear and opening) across crack faces. Internal nodes do not show up in the global stiffness matrix for finite element analysis, allowing the flexibility of adding them or removing them in any element without affecting the overall analysis. An advantage of SDA and therefore EDM over more conventional discrete crack models, such as cohesive crack interface element models, is that it allows cracks to propagate through elements, in other words, independent of nodal positions and element boundaries. EDM differs from so-called smeared crack or crack band approaches in that it forms a discontinuous cracked surface, rather than an overstretched band of elements. The use of displacement rather than strain to enforce softening has as important advantage that EDM does not suffer from mesh size dependencies.

The constitutive equations of the EDM formulation used for the present paper were published elsewhere [12]. The methodology uses the efficient crack adaptation technique to prevent crack locking developed by Sancho et al [10]. In the earlier work [12] a simple exponential softening relation for crack damage evolution was used for both shear and opening mode fracture. The simple exponential softening function is not suitable for the simulation of fracture in fibre reinforced concrete. The exponential shape will result in too much energy being dissipated in the initial stage of softening, leading to an overprediction of the experimental peak load [2]. The distinct post crack tension behaviour of fibre reinforced concrete with the initial spike in strength followed by gradual softening at a lower stress necessitated the selection of a more appropriate shape of the softening function.

3.2 Exponential softening function with crack tip singularity

The post cracking softening behaviour of plain concrete is often modelled using a bilinear function. For example, Guinea et al [13] proposed a model using four parameters, i.e.: f_t, G_f and two parameters dependent on the shape of the function determined from experimental results. Recently, Park et al [14] proposed a two parameter model.

Compared to plain concrete FRC has an significantly extended post crack softening process. An early bilinear cohesive crack model for fibre reinforced concrete by Hillerborg [15] proposed an initial softening slope equal to that of plain concrete followed by a kink and a stable stress plateau. In recent work, more complex tri-linear shapes of the softening function have been proposed for fibre reinforced concrete by various researchers [16], [17], [18], [19].

Research on concrete with similar steel fibres from the same producer as used in this study has shown that when a crack forms the stress transferred across the crack drops rapidly until it stabilizes

at a lower stress it then softens further at a slower pace [16]. Based on this work, Lim et al [16] proposed a softening function with a crack tip singularity to simulate the behaviour of the material in tension. Such a curve with an initial spike at high strength followed by a long tail at a lower stress is suitable for fibre reinforced composites, as it simulates the initial failure of the matrix followed by the slow pull out of the fibres [1], [20]. In this paper the post crack behaviour of the material is simulated using a softening function with crack tip singularity followed by exponential softening. The material behaviour in tension is shown schematically in Figure 6a. Initially the material behaves linear elastically until f_t, is reached. At this point a crack is introduced in the concrete causing the stress to drop until the fibres are activated. In the model it is assumed that the stress drops without an increase in crack width w, resulting in a crack tip singularity. The stress at the base of the singularity is the post singularity crack bridging stress (σ_1). After the initial drop in stress, the softening takes an exponential form. The proposed shape is based on an assessment of the data presented by Lim et al [16]. No physical testing to determine the shape of the softening function was performed as part of this study. The value of σ_1 is obtained through empirical calibration, the validity of the calibration has to be checked by comparing the results for different specimen sizes and/or geometries.

To achieve the material behaviour shown in Figure 6a, a softening relation combining a linear and an exponential part was implemented in the finite element code. The relation is as shown in Figure 6b. When the tensile strength (f_t) of the material is reached a crack is formed, the stress transferred across the crack reduces linearly with an increase in crack width (w) for $0 < w < w_1$ according to:

$$\sigma = f_t \left(\frac{f_t - \sigma_1}{w_1} \right) w \tag{12}$$

Once w_1 is reached softening becomes exponential for $w_1 < w < \infty$. The exponential softening is defined by value of σ_1 and the remaining fracture energy $G_{f,1}$. This is the specific fracture energy G_f less the energy dissipated under the linear softening:

$$G_{f,1} = G_f - \left(\frac{f_t + \sigma_1}{2} \right) w_1 \tag{13}$$

The exponential part of the softening function is given by:

$$\sigma_w = \sigma_1 e^{(-a_1(w-w_1))} \tag{14}$$

With:

$$a_1 = \frac{\sigma_1}{G_{f,1}} \tag{15}$$

To create the softening curve with crack tip singularity shown in Figure 6a, w_1 was set to 0 in the softening function of equations 12, 13 and 14. As G_f is determined from the TPB results and f_t is obtained from tensile splitting tests as discussed in Section 4, σ_1 is now the only unknown to be calibrated in the model.

4. Experimental setup

Laboratory testing was performed on specimens produced from two high performance concrete mixes. The mix designs are both typical for the material used in UTCRCP construction, but differ significantly in composition and material properties. Mix A was prepared with 80 kg/m^3 steel fibres, Mix B with a steel fibre content of 120 kg/m^3. Apart from steel fibres which are added to impede macro cracking, the mixes contain synthetic fibres to provide the material with resistance against micro cracking. The mix designs are shown in Table 1.

The engineering properties obtained for the concrete mixtures are shown in Table 2. The compressive strength (f_c) of the material was determined in accordance with British Standard BS 1881 [21]. The ASTM C469-02 [22] standard procedure was used to obtain the static modulus of elasticity (E) in compression and Poisson's ratio v for the material. A best estimate of the tensile strength (f_t) was determined using the cylinder splitting test. In the splitting tests the recommendations for the reduction of the size effect made by Rocco et al [23], in terms of loading speed and width of the loading strip were observed. All tests were performed after 28 days of water curing.

A set of three beams was produced from Mix A. The specimen dimensions are shown in Table 3. The objective of this set of tests was to validate the methodology to measure G_f as presented in Section 2 of this paper. The specimens cast from mix B were part of a study on size-effect in fibre reinforced concrete [2]. For this purpose, beam specimens of three different sizes were cast while maintaining the geometry as shown in Table 3. The depth to span and notch to depth ratios were kept constant for all specimen sizes. The loading apparatus, loading speed, arrangement of deflection and CMOD gauges, loading device and roller support for all test complied with the recommendations for bending tests as provided by RILEM TC 162-TDF [24].

5. Finite element model

The EDM was implemented using three-node triangular elements. A typical example of a two dimensional mesh used in the simulation of the TPB tests is shown in Figure 7. In principle it is possible to use embedded discontinuity elements for the entire geometric model. This will allow the crack to form at the position in the specimen with the highest tensile stress. In simulation of the notched TPB tests however, the crack will always form directly above the notch. Therefore, to save

on calculation time, the elements with embedded discontinuity were arranged in a vertical band above the notch as shown in the figure. A characteristic length of 1.0 mm was used for the EDM elements in the analysis of all specimens. The remainder of the material is modelled using linear elastic (LE) bulk elements.

6. Results

The load-deflection curves for the different specimen types are shown in Figure 8. The results of the numerical analysis and the deformed mesh are also shown in the figure. The fracture energy was determined from the experimental load-deflection curves in accordance with the procedure introduced in Section 2 of this paper. The results for parameter A, the work of fracture W_f and the percentage of W_f under the tail are shown in Table 4. According to the proposed model, approximately 18 per cent on average of the work of fracture was still available from the beams when the tests were stopped. The overall average coefficient of variation for the G_f values is 10 per cent, which is considered to be acceptable. The table also shows the nominal tensile strength σ_{Nu} for the beams calculated under the assumption of a linear elastic stress distribution in the section:

$$\sigma_{Nu} = \frac{3P_u s}{2bh^2} \tag{16}$$

Where P_u is the peak load recorded during the test. A statistically significant size-effect is present in the σ_{Nu} results for the TPB tests on Mix B specimens. The results obtained in this study do not indicate a statistical size-effect in the value of G_f. Due to the variability inherent to the material and TPB results, a large number of specimens would have to be tested in order to verify whether size-effect in G_f occurs.

With both the f_t and G_f known for the two mixes, the softening curves can be constructed. Figure 9 shows the calibrated softening curves for the two mix types. Due to differences in mix composition and importantly fibre content, Mix B has a higher post crack tensile capacity than Mix A for any value of w. The difference between the mixes in terms of post cracking stress transfer capacity is visible in the figure.

For Mix A, the value of σ_1 was picked by means of a parameter study, such that it yields the best fit to data for the numerical simulation of the TPB results shown in Figure 8a. The resulting softening function allows a satisfactory simulation of the fracture behaviour of the UTCRCP material. For Mix B the softening curve was constructed using the G_f data for specimen type TPB-II-B. The value of σ_1 was calibrated for this specimen type and then applied to predict the fracture behaviour of the two remaining specimen types. The results were satisfactory, indicating that the calibration is justified.

Figure 10 shows a comparison between the σ_{Nu} values obtained for the experimental and simulated load-deflection curves for Mix B. The numerical simulation predicts the occurrence of size-effect size effect. The size effect in the experimental results is stronger however than predicted by the numerical simulation. This is due to the fact that the numerical simulation predicts fracture mechanics size effect only. Other sources of size-effects stemming from specimen preparation, e.g the boundary layer effect, the statistical size effect, size related differences in hydration heat, etc. are not predicted in the numerical analysis.

4. Conclusions

The objective of this paper is to numerically simulate opening mode fracture in high performance fibre reinforced concrete road pavement materials. A simple, but effective methodology was

presented to predict the fracture behaviour of the material in flexure, using a fracture mechanics approach.

The fracture energy (G_f) of the material is determined from three point bending (TPB) experiments. TPB tests on fibre reinforced concrete are invariably stopped before the specimen is fully broken. An extrapolation technique is proposed that allows the extension of the load displacement curves and determine the full work of fracture (W_f) required to break the beam specimens completely. A best estimate of G_f can then be calculated from the W_f values thus obtained.

The post crack softening behaviour of the material is described using a cohesive crack softening relation which combines crack tip singularity with an exponentially softening tail. The shape of the softening function is defined by three parameters, i.e. G_f, the tensile strength (f_t) and a third parameter σ_1 representing the crack bridging stress at the base of the singularity, which is obtained through calibration.

Numerical simulation of the TPB experiments is performed using an embedded discontinuity method (EDM) implemented into an open source finite element software framework. Damage evolution in the EDM takes place according to the softening function with crack tip singularity. The numerical model allows satisfactory simulation of the opening mode fracture behaviour of the material in three point bending (TPB) experiments.

The TPB experiments performed on geometrically similar specimens of different sizes confirm that the high performance fibre reinforced concrete under study is subject to significant size effect. The nominal tensile strength (σ_{Nu}) calculated for a certain beam size can therefore not be used to reliably predict the peak load of specimens of a different size using linear elastic (LE) theory. It follows that such LE analysis cannot be expected to yield reliable predictions of the bending capacity of a full size road pavement slab. In contrast, the fracture mechanics based methodology applied in this paper

allows the prediction of size effect in the TPB experiments. The ability of the method to simulate the fracture behaviour of specimens of different sizes shows that the calibration of σ_1 is justified. It is recommended that the suitability of the method to predict the flexural capacity of full size high performance fibre reinforced pavement slabs is investigated.

References

[1]   Bažant ZP, Planas J. Fracture and size effect in concrete and other quasibrittle materials. CRC Press; 1997.

[2]   Denneman E, Kearsley EP, Visser AT. Size-effect in high performance concrete road pavement materials. In: Van Zijl GPAG, Boshoff WP, editors. Advances in cement-based materials, London: CRC Press; 2010, p. 53-58.

[3]   Elices M, Guinea GV, Planas J. Measurement of the fracture energy using three-point bend tests: Part 3 – Influence of cutting the P-δ tail. Mater and Struct 1992;25:327-334.

[4]   Elices, M, Guinea GV, Planas J. On the measurement of concrete fracture using the three-point bend test. Mater and Struct 1997;30:375-376.

[5]   Rosselló C, Elices M, Guinea GV. Fracture of model concrete: 2. Fracture energy and characteristic length. Cement Concrete Res 2006;36:1345-1353.

[6]   Hillerborg A, Modéer M, Petersson P-E. Analysis of crack formation and crack growth in concrete by means of fracture mechanics and finite elements. Cement Concrete Res 1976;6:773-782

[7]   Simo J, Oliver J, Armero F. An analysis of strong discontinuities induced by strain-softening in rate-independent inelastic solids. Computational Mech 1993;12;5:227-296.

[8]   Oliver J. Modelling strong discontinuities in solid mechanics via strain softening constitutive equations. Part 1: fundamentals. Int J Numerical Methods in Engng 1996;39;21:3575-3600.

[9]   Oliver J 1996, Modelling strong discontinuities in solid mechanics via strain softening constitutive equations. Part 2: numerical simulation, Int J Numerical Methods in Engng 1996;39;21:3601-3623.

[10]   Sancho JM, Planas J, Cendón DA, Reyes E, Gálvez JC. An embedded crack model for finite element analysis of concrete. Engng Frac Mech 2007;74:75-86.

[11]   OpenSees. Open System for Earthquake Engineering Simulation. v1.7.5. Berkeley: Pacific Earthquake Engineering Research Center University of California; 2008.

[12]   Wu R, Denneman E, Harvey JT., Evaluation of Embedded Discontinuity Method for Finite Element Analysis of Cracking of Hot-Mix Asphalt Concrete. Transportation Res Record 2009;2127:82-89.

[13]   Guinea GV, Planas J, Elices M. A general bilinear fit for the softening curve of concrete. Mater and Struct 1994;27:99-105

[14] Park K, Paulino GH, Roesler JR. Determination of the kink point in the bilinear softening model for concrete. Engng Fracture Mech 2008;75:3806-3818.

[15] Hillerborg A. Determination and significance of the fracture toughness of steel fibre concrete. In: Shah, SP, Skarendahl A, editors. Steel fiber concrete US-Sweden joint seminar, Elsevier Applied Science Publishers, London; 1986, p 257–271.

[16] Lim T, Paramasivam P, Lee S., Analytical model for tensile behavior of steel-fiber concrete. ACI Mat J 1987;84:286-298.

[17] Pereira EN, Barros JA, Ribeiro AF, Camões A. Post-cracking behaviour of selfcompacting steel fibre reinforced concrete. In Proceedings of the 6th International RILEM Symposium on Fibre Reinforced Concrete - BEFIB 2004, Varenna; p. 1-10

[18] RILEM TC 162-TDF: 'Test and design methods for steel fibre reinforced concrete' σ-ε-design method. Mat Struct 2003;36:560-567.

[19] Roesler JR, Paulino GH, Gaedicke C, Bordelon A, Park K. Fracture Behavior of Functionally Graded Concrete Materials for Rigid Pavements. Transportation Res Record 2007; 2037:40-49.

[20] Dupont D, Vandewalle L. Comparison between the round plate test and the RILEM 3-point bending test. In Proceedings of the 6th International RILEM Symposium on Fibre Reinforced Concrete - BEFIB 2004, Varenna; p. 101-110

[21] BS 1881: Testing concrete. Part 116: 1983 Method for determination of compressive strength of concrete cubes. British Standard Institute; 1983.

[22] ASTM C469-02. Standard Test Method for Static Modulus of Elasticity and Poisson's Ratio of Concrete in Compression. Annual book of ASTM standards 2008: section 04.02. Washington; 2008.

[23] Rocco C, Guinea GV, Planas J, Elices M. Size effect and boundary conditions in the Brazilian test: Experimental verification. Mater and Struct 1999;32:210-217.

[24] RILEM TC 162-TDF: Test and design methods for steel fibre reinforced concrete; bending test. Mat Struct 2002;35:579-582.

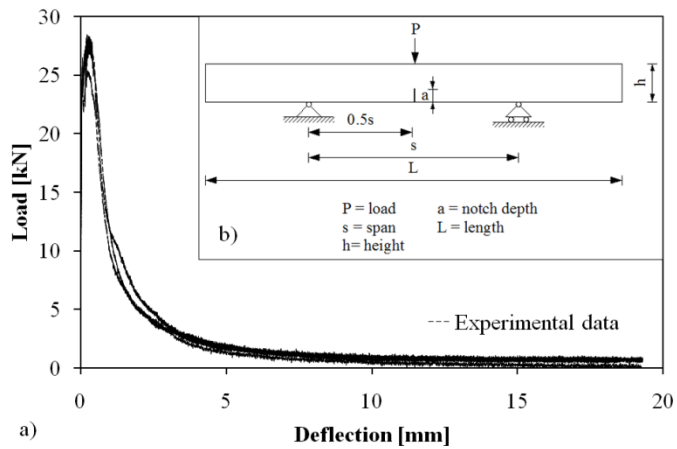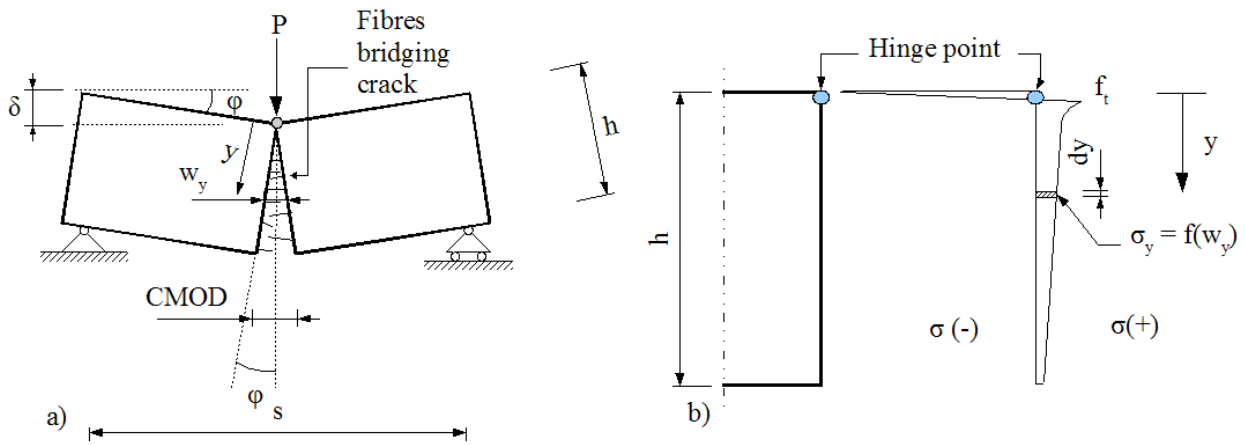**Figure 1a: Load-deflection curve for TPB test, b: TPB test configuration**

Figure 2a: Kinematic model of TPB test at large deflections, b: Stress distribution in kinematic model (not to scale)
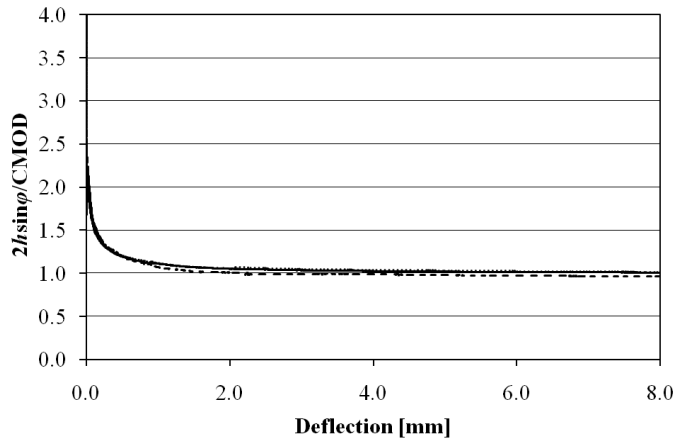
Figure 3: Comparison of recorded CMOD and crack mouth opening calculated using the kinematic model in Figure 2.
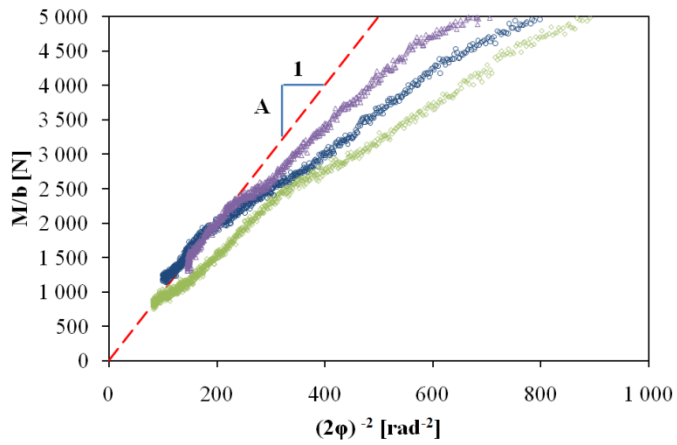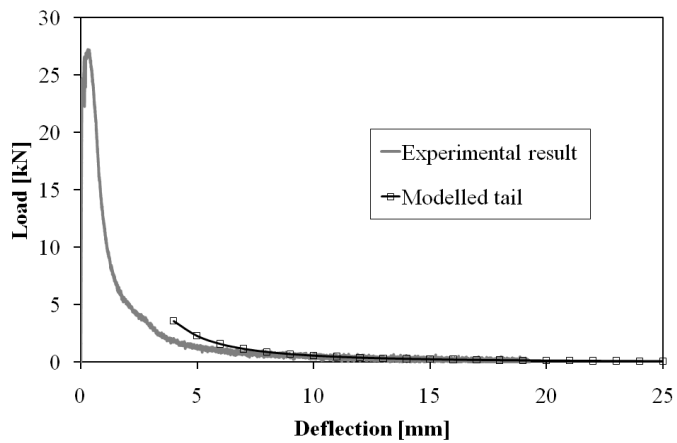

Figure 4: Determination of parameter A.

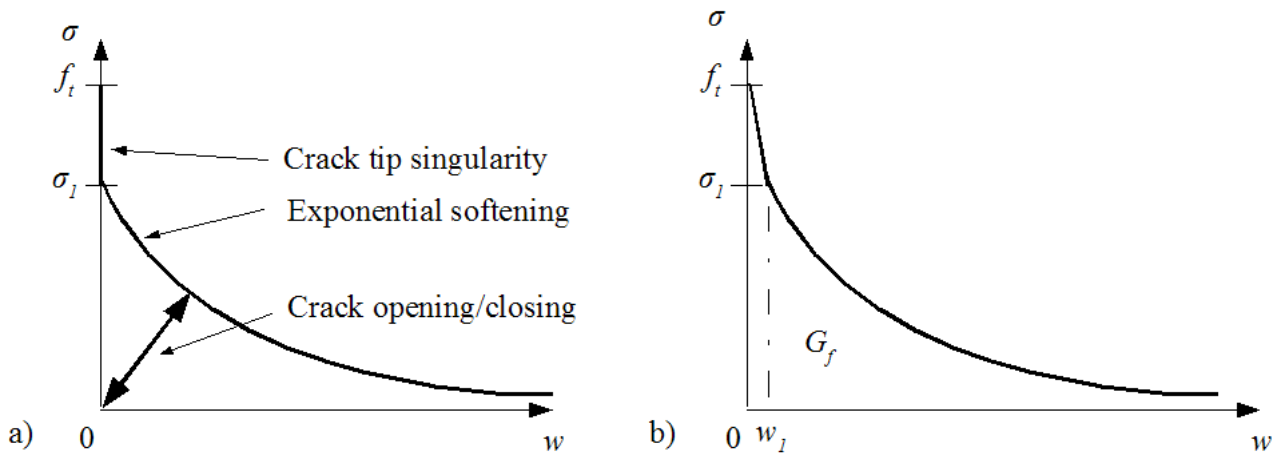**Figure 5: Load deflection curve with modelled tail.**

Figure 6a: Material behaviour in simulation, b: Softening function as implemented in FEM code (w_1 is set to 0 to achieve the behaviour shown in Figure 6a)
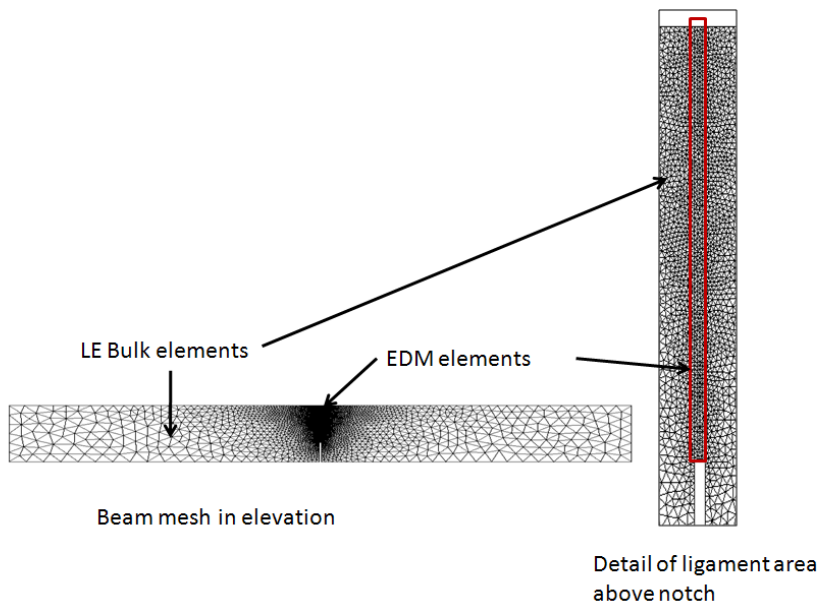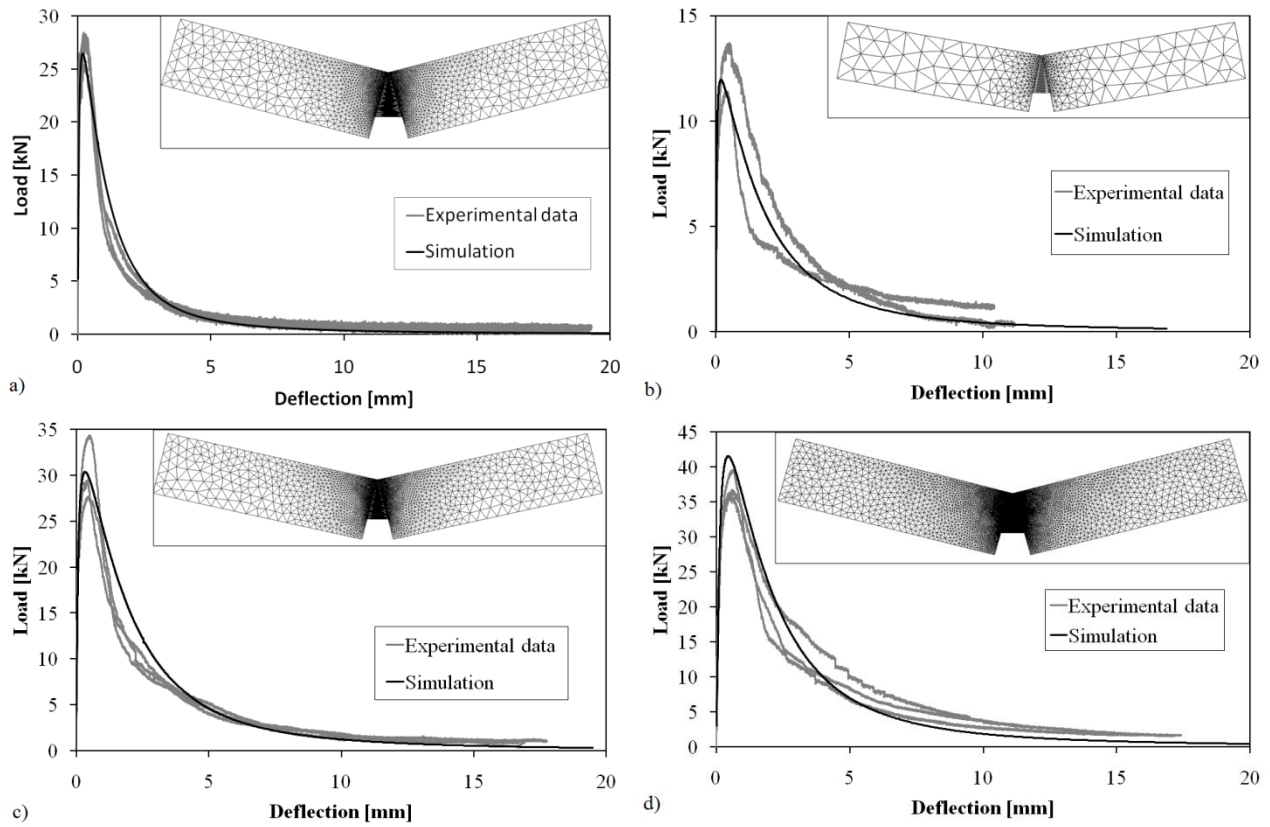

Figure 7: Finite element mesh

Figure 8: Comparison of experimental and simulated load-deflection response for: a) beam type TPB-I-A, b) beam type TPB-I-B, c) beam type TPB-II-B, and d) beam type TPB-III-B
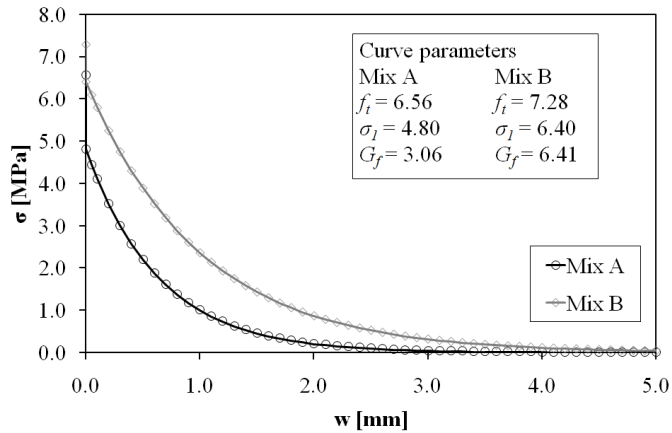

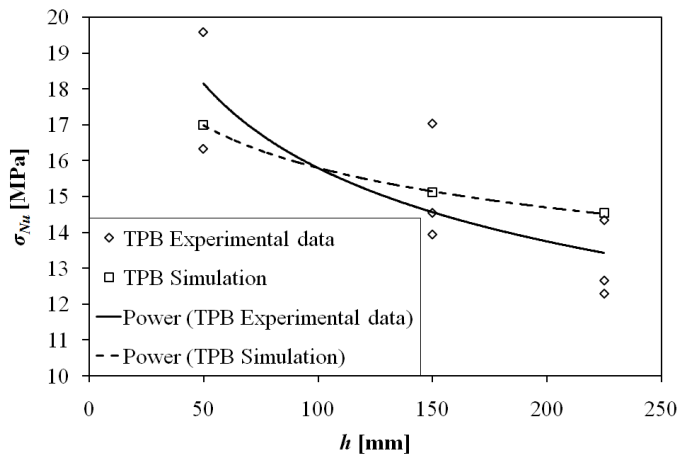**Figure 9: Optimized softening functions for studied mixes.**

Figure 10: σ_{Nu} **size-effect as observed in experiments and predicted in simulation**

Table 1: Mix designs

Component	Description	Mix A [kg/m^3]	Mix B [kg/m^3]
Cement	Cem I 52.5 N	450	465
Coarse aggregate	6.7mm[a]	950	866
Fine aggregate	4.75mm[a]	900	751
Water	Tap water	165	176
Steel fibres	Baekert Dramix [30 mm x 0.5 mm]	80	120
Synthetic fibre	Polypropylene [12 mm]	2.0	2.0
Admixture	P100 and O100	8.0	7.4
Silica Fume (CSF)	Witbank	50	64
Fly ash (PFA)	Lethabo	0	79

[a] Dolomite aggregate was used for mix A, Quartzite was used for mix B

Table 2: Engineering properties

Material property		Unit	Mix A		Mix B	
			Value	Std.dev.	Value	Std.dev.
Compressive strength	f_c	MPa	137.2	6.0	125.5	4.7
Modulus of elasticity	E	GPa	62.9	0.7	49.7	0.7
Poisson's ratio	υ		0.15	0.005	0.17	0.005
Tensile strength	f_t	MPa	6.56	0.73	7.28	0.51

Table 3: Specimen dimensions

Type	Width b [mm]	Height h [mm]	Length L [mm]	Span s [mm]	Notch depth a [mm]	Number of successful tests
TPB-I-A	150	150	900	450	50	3
TPB-I-B	150	50	330	165	16.5	2
TPB-II-B	150	150	1000	500	50	3
TPB-III-B	150	225	1500	750	75	3

Table 4: Measured fracture properties

Specimen type	A [N]	W_f [Nmm]	W_{tail} [%]	G_f [N/mm] Value	G_f Std.dev.	σ_{Nu} [MPa] Value	σ_{Nu} Std.dev.
TPB-I-A	11.6	5.43E+05	19.0	3.06	0.50	10.9	0.81
TPB-I-B	14.0	4.26E+04	19.2	8.34	0.24	17.9	2.3
TPB-II-B	11.4	9.66 E+04	15.0	6.41	0.63	15.2	0.43
TPB-III-B	15.2	1.62 E+04	17.8	7.41	0.86	13.1	1.45